Eur. Phys. J. A **7**, 537–541 (2000)

THE EUROPEAN PHYSICAL JOURNAL A

Near-threshold η production in the $p\,d \longrightarrow p\,d\,\eta$ reaction

F. Hibou[1], C. Wilkin[2], A.M. Bergdolt[1], G. Bergdolt[1], O. Bing[1], M. Boivin[3], A. Bouchakour[1], F. Brochard[3,6], M.P. Combes-Comets[4], P. Courtat[4], R. Gacougnolle[4], Y. Le Bornec[4], A. Moalem[5], F. Plouin[3,6], F. Reide[4], B. Tatischeff[4], N. Willis[4]

[1] Institut de Recherches Subatomiques, IN2P3-CNRS/Université Louis Pasteur B.P. 28, 67037 Strasbourg Cedex 2, France
[2] University College London, London WC1E 6BT, UK
[3] Laboratoire National Saturne, 91191 Gif-sur-Yvette Cedex, France
[4] Institut de Physique Nucléaire, IN2P3–CNRS/Université Paris-Sud, 91406 Orsay Cedex, France
[5] Physics Department, Ben Gurion University, 84105 Beer Sheva, Israel
[6] LPNHE, Ecole Polytechnique, 91128 Palaiseau, France

Received: 23 March 2000
Communicated by J. Äystö

Abstract. The total cross section of the $p\,d \rightarrow p\,d\,\eta$ reaction has been measured at two energies near threshold by detecting the final proton and deuteron in a magnetic spectrometer. The values are somewhat larger than expected on the basis of two simple theoretical estimates.

PACS. 13.60.Le Meson production – 25.10.+s Nuclear reactions involving few-nucleon systems – 25.40.Ve Other reactions above meson production thresholds (energies > 400 MeV)

1 Introduction

The production of η mesons in the $p\,d \rightarrow {}^3\mathrm{He}\,\eta$ reaction near threshold is remarkable for both its strength and its energy dependence [1,2]. The threshold amplitude is of a similar size to that for pion production, despite the much larger momentum transfers associated with η formation. Although the angular distribution remains isotropic, suggesting S-wave production, the square of the amplitude falls by a factor of three over a 5 MeV change in the c.m. excess energy Q. This has been taken as indicative of a nearby quasi-bound state of the $\eta\,{}^3$He system, arising through strong η multiple scatterings from the three nucleons in the recoiling nucleus [3].

In order to transfer such large momenta, Kilian and Nann [4] suggested two-step processes involving intermediate pions. They showed that the threshold kinematics for $p\,d \rightarrow {}^3\mathrm{He}\,\eta$ were in a sense *magic*. The momentum of the η produced in the reaction is very similar to that obtained from the sequential physical processes of $pp \rightarrow d\pi^+$ followed by $\pi^+ n \rightarrow p\eta$, when there is no relative momentum between the final $p\,d$ pair and all Fermi momenta are neglected. In such cases the final proton and deuteron are likely to stick to form the observed ^{3}He nucleus. The classical estimate of the enhancement due to the magic kinematics is broadly confirmed by quantum mechanical calculations [5], which reproduce the size of the near-threshold cross section to within about a factor of two.

The same two-step model should also be capable of explaining events where the final proton and deuteron emerge freely in the $p\,d \rightarrow p\,d\,\eta$ reaction and the aim of the present investigation was to undertake a first exploration of this cross section near the threshold beam energy of $T_p = 901.2$ MeV. Unfortunately, due to the closure of the laboratory, data could only be obtained at two beam energies.

2 Experiment

The experiment was carried out at the Laboratoire National SATURNE (LNS), using the large acceptance magnetic spectrometer SPESIII, which was well adapted for the study of meson production in three-body final states near threshold through the detection of two charged particles. The experimental conditions concerning the beam monitoring, particle detection and identification, were rather similar to those of previous studies of meson production in the $p\,p \rightarrow p\,p\,X$, where the meson X was identified by the missing mass method [6]. A liquid deuterium target of 207 mg/cm^2 thickness was employed and, in order to improve the missing mass resolution and the signal-to-background ratio, the opening of the vertical collimators of SPESIII was reduced to $\pm$40 mr.

One special feature of the $p\,d \rightarrow p\,d\,\eta$ reaction near threshold is the low momentum, around 400-500 MeV/c, of the outgoing proton. This is to be compared with

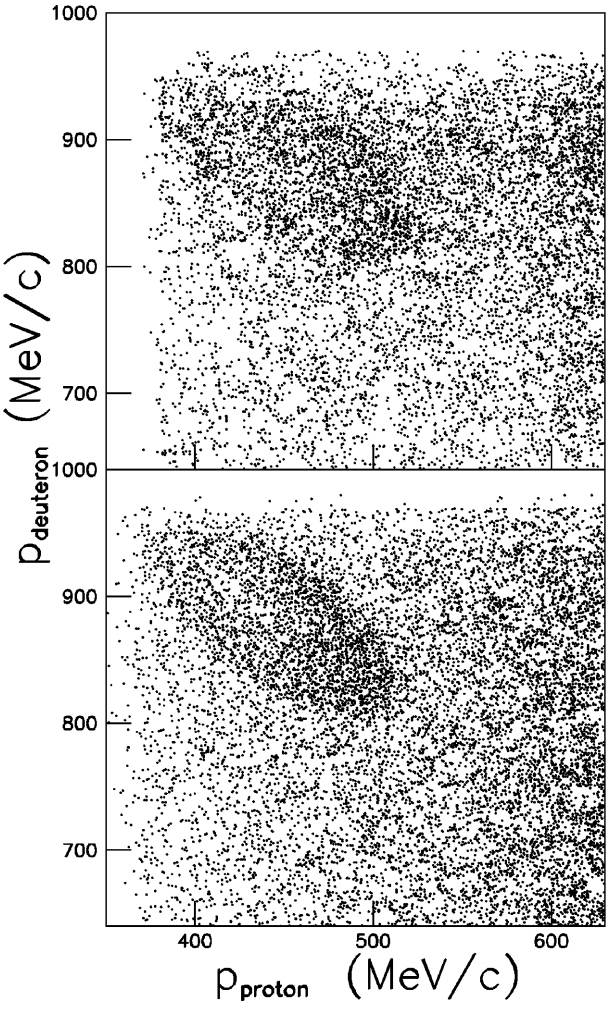

Fig. 1. Two-dimensional scatter plot of the momenta of the proton and deuteron arising from the reaction $p\,d \to p\,d\,X$ a little above the η threshold. The experimental data, shown in the upper figure, were measured at a nominal beam energy $T_p = 909$ MeV but, as discussed in the text, this is expected to be 1-2 MeV above the true value. The simulation in the lower figure was carried out at 907 MeV. Events from the $p\,d \to p\,d\,2\pi$ reaction populate the whole plot but in the top left corner one can see an ellipse containing extra events corresponding to η production

the standard 600-1400 MeV/c momentum range of the SPESIII spectrometer. The momentum of the recoiling deuteron is about 900 MeV/c and, in order to detect both particles simultaneously, the magnetic field was tuned down to accept momenta from about 360 to 960 MeV/c. Under normal SPESIII working conditions, the values of the particle momenta were obtained by using well established polynomial relations, taking the coordinates of the trajectories near the focal surface as input. The properties of SPESIII were not extensively studied with reduced fields and, in the present experiment, we used the polynomial parametrisation with the momenta of the particles scaled according to the ratio of the actual to the standard mean field, (2.03 Tesla)/(3.07 Tesla). This procedure essentially assumes that the field was reduced uniformly. A similar method was applied in the simulations, applying the same ratio to the momenta when tracking the particles. Such simulations are important for generating the expected missing mass peak of the $p\,d \to p\,d\,\eta$ reaction as well as the background spectrum of the $p\,d \to p\,d\,2\pi$ reaction.

Two-dimensional experimental and simulated scatter plots of the emerging proton and deuteron momenta are shown in Fig. 1. Superimposed upon a fairly uniform background, due the $p\,d \to p\,d\,2\pi$ reaction, there is a darker ellipse inside which the $p\,d \to p\,d\,\eta$ events are confined. The experimental missing mass spectra of the $p\,d \to p\,d\,X$ reaction are shown in Figs. 2a1 and 2a2. Clear η peaks are observed near the upper edges of phase space for the two nominal proton beam energies of 905 and 909 MeV. Simulated background spectra of the $p\,d \to p\,d\,2\pi$ reaction are shown in Figs. 2b1 and 2b2 and simulated peaks of the $p\,d \to p\,d\,\eta$ reaction are represented by the solid lines in Figs. 2c1 and 2c2. To evaluate the number of $p\,d \to p\,d\,\eta$ events, the two simulated spectra were combined so as to fit the experimental data. After subtracting the simulated background from the experimental results, the remaining events (points with error bars) in Figs. 2c1 and 2c2 show good agreement with the simulated $p\,d \to p\,d\,\eta$ spectra (solid line).

Taking the mass of the η meson to be 547.30 MeV/c^2 [7], the best fits were obtained by assuming incident proton energies which were 1-2 MeV lower than the nominal values derived from the Saturne machine parameters. The fits also suggested adjusting the mean field ratio to a value slightly below that of the initial 2.03/3.07 *ansatz*. However, due to the uncertainties in the effective field strength and the particle tracking, no definitive accurate values of the beam energies could be deduced from the fitting procedure. But, since the shift indicated here is very similar to the mean difference $\Delta T = T_{\rm nominal} - T_{\rm measured} = 1.1 \pm 1.0$ MeV obtained at Saturne from other meson-production reactions near threshold [6,8,9], we adopt this energy correction ΔT, to be subtracted from the nominal values to obtain the 'true' ones. The average values of the excess energies $Q = \sqrt{(m_p + m_d)^2 + 2m_d T_p} - m_p - m_d - m_\eta$, where the m_i are particle masses, were determined using the corrected proton energies and taking into account energy losses in the target. These energies were used in the simulations required to evaluate the SPESIII acceptances, which were estimated assuming phase-space distributions of final particles. The acceptance decreases very quickly above threshold through one of the final particles falling outside the solid angle of SPESIII. Nevertheless, from the resulting angular dependence of the acceptance shown in Fig. 3 as a function of the cosine of the η emission angle in the centre-of-mass system, it can be seen that all the regions of phase space were covered. The resulting overall acceptances of 24% and 7%, evaluated at the mid-target energies of $T_p = 903.7$ and 907.7 MeV respectively, lead to the cross sections given in Table 1. The first error on the cross sections given in the table includes the statistical error (10% and 18% respectively) and a 13% systematic error on the absolute normalisation. The ±0.6 MeV un-

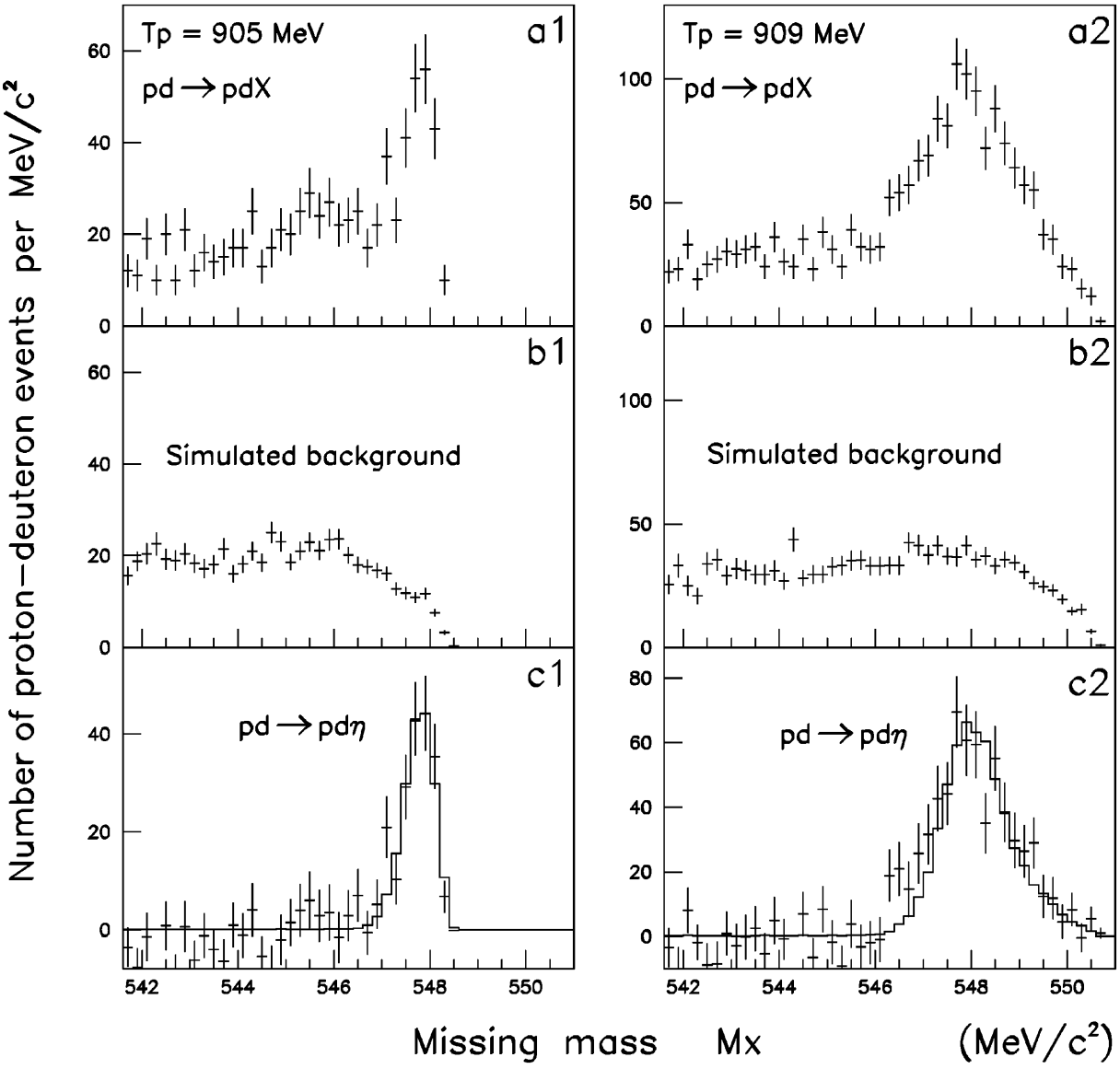

Fig. 2. Missing mass spectra of the $p\,d \to p\,d\,X$ reaction at nominal beam energies of (1) 905 MeV, and (2) 909 MeV. The observed spectra in (a1) and (a2) are to be compared with background spectra $p\,d \to p\,d\,2\pi$ in (b1) and (b2) estimated by Monte Carlo simulation. The shapes and widths of the η peaks, found by subtraction and shown in (c1) and (c2), are in good agreement with the Monte Carlo predictions (solid lines) assuming true beam energies 1-2 MeV below the nominal values suggested by the macroscopic parameters of Saturne

certainty in Q gives rise to the additional quoted errors through the rapid acceptance variation. However, the latter errors affect little the comparison with theory since, if both values of Q are increased by 0.6 MeV, the experimental points move largely in the directions given by the theoretical curves. Due to its slow energy variation, the proton-deuteron final state interaction is unlikely to affect the acceptance evaluation. However, if η rescattering were to distort sharply the shapes of the final proton-deuteron distributions, then this could have an effect. In view of the reasonable agreement with our phase space Monte Carlo simulation found in the two-dimensional plot of Fig. 1, any effect is likely to be small, but cannot be fully quantified without more refined measurements.

3 Comparison with theory

Estimates have been made of the $p\,d \to p\,d\,\eta$ total cross section near threshold in the quantum two-step model of [10], though neglecting all final state interactions. The energy variation of

$$\sigma_T(pd \to pd\eta) = 1.2\,Q^2 \text{ nb} \qquad (1)$$

is compatible with that of our data shown in Fig. 4. The predicted values of 2.7 and 17 nb, at $Q = 1.5$ and 3.8 MeV respectively, are only about a factor of two smaller than our results and this discrepancy could be due to the neglect of the strong final state interaction between the proton and deuteron.

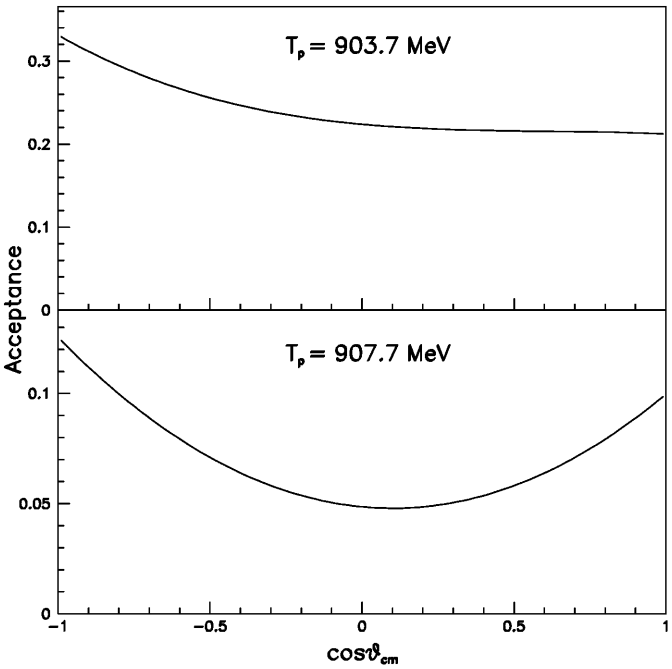

Fig. 3. Acceptance of the SPESIII spectrometer for the reaction $p\,d \to p\,d\,\eta$ at mid-target beam energies of 903.7 and 907.7 MeV as a function of the cosine of the η production angle in the centre-of-mass system. The curves have been calculated assuming phase-space distributions

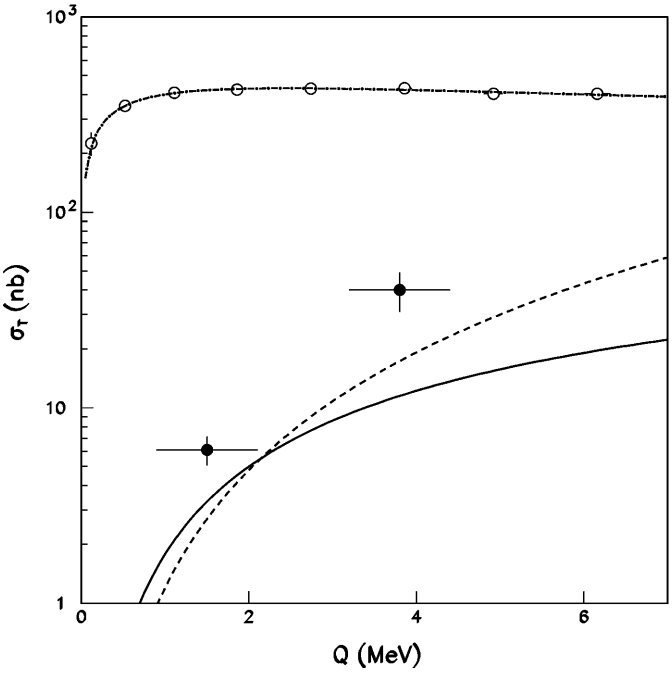

Fig. 4. Measured total cross sections for the $p\,d \to p\,d\,\eta$ reaction close to threshold. The additional errors arising from the influence of the uncertainty in the absolute value of Q given in Table 1 are not indicated since, due to the $Q-\sigma$ error correlation, they have much smaller components perpendicular to the theoretical predictions. The solid curve is the prediction for the spin-$\frac{1}{2}$ final state in the final-state-interaction model of (2) [12]. The dashed curve has been estimated in the two-step model of [10], where final state interactions have been neglected. The $pd \to {}^3\mathrm{He}\,\eta$ data of [2] and the parametrisation of (3) are shown by the open circles and dot-dashed curve respectively

Table 1. Measured total cross sections for the $p\,d \to p\,d\,\eta$ reaction at a mid-target centre-of-mass excess energy Q. Although there are ± 0.6 MeV uncertainties in the values of Q, the relative value is correct to ± 0.1 MeV. The first quoted error in the cross sections includes statistical and normalisation uncertainties; the second is that induced by the uncertainty in Q. For the first point the energy uncertainties are negligible for σ/Q, whereas for the second point it is σ/Q^2 which is largely unaffected by ΔQ.

Q (MeV)	$\sigma_T(pd \to pd\eta)$ (nb)
1.5 ± 0.6	$6.1\pm1.0\pm^{2.8}_{2.0}$
3.8 ± 0.6	$40\pm9\pm^{13}_{10}$

There are two possible S-wave proton-deuteron final states, corresponding to spin $\frac{1}{2}$ and $\frac{3}{2}$. The low energy spin-quartet scattering wave functions show little structure at short distances, whereas the spin-doublet bear some similarity to the shape of the $p\,d$ distribution at short distances inside the bound ^{3}He nucleus [11].

The connection between the bound and scattering $p\,d$ wave functions can be exploited to estimate the production of η mesons in the $p\,d \to p\,d\,\eta$ reaction, with the final $p\,d$ system in the spin-$\frac{1}{2}$ state, in terms of the cross section for $p\,d \to {}^3\mathrm{He}\,\eta$. Provided that the structure of the deuteron is neglected, the relative normalisation of the bound and scattering wave functions at short distances is fixed purely by the proton-deuteron binding energy, $\epsilon \approx 5.5$ MeV, in the ^{3}He nucleus. If the meson production operator is also of short range, the production in two and three-body final states should be related through [12]

$$\sigma_T(pd \to pd\eta) = \frac{1}{4}\left(\frac{Q}{\epsilon}\right)^{3/2}\left(1+\sqrt{1+Q/\epsilon}\right)^{-2} \times \sigma_T(pd \to {}^3\mathrm{He}\,\eta)\,. \quad (2)$$

This approach [12] reproduces about $\frac{2}{3}$ of the $p\,d \to p\,d\,\pi^0$ total cross section [13] in terms of that for $p\,d \to {}^3\mathrm{He}\,\pi^0$ [14] and the residue could be due to spin-$\frac{3}{2}$ final states.

The very precise near-threshold $p\,d \to {}^3\mathrm{He}\,\eta$ total cross section data [2] may be parametrised as

$$\sigma_T(pd \to {}^3\mathrm{He}\,\eta) = \left(\frac{p_\eta}{p_p}\right)\frac{22}{(1+1.6p_\eta)^2+(3.8p_\eta)^2}\ \ \mu\mathrm{b}\,, \quad (3)$$

where the η and proton c.m. momenta p_η and p_p are measured in fm^{-1}. This parametrisation is shown in Fig. 4.

The predictions of (2) for the $p\,d \to p\,d\,\eta$ total cross sections are about a factor of three lower than our experimental results shown in Fig. 4. This may be due to the short-range assumption for the meson-production op-

erator made in deriving (2). In the two-step model of [5], the momentum transfer is provided through having a secondary interaction with an intermediate pion. Since high Fermi momenta are then not required, this means that the final $p\,d$ system is not necessarily produced at short distances. However, at larger distances the scattering wave functions are generally bigger than bound state ones, which must die off exponentially. It would therefore be very desirable to have a microscopic two-step model calculation of the type of [10] but with the proton-deuteron final state interaction included.

4 Summary

We have made the first measurements of the $p\,d \to p\,d\,\eta$ reaction near threshold and obtained cross sections about a factor of 2-3 higher than those of two simple theoretical approaches. Since, for our data, Q is less than the ^{3}He binding energy ϵ, the difference in the energy dependence of the two present models comes principally from the striking behaviour of the $pd \to {}^3\mathrm{He}\,\eta$ cross section. More detailed experiments, with a much better resolution in Q, are required to see if there is in fact a strong η final state interaction in the $p\,d\,\eta$ system to match that in $^3\mathrm{He}\,\eta$.

We wish to thank the Saturne accelerator crew and support staff for providing us with working conditions which led to the present results. Discussions with U. Tengblad regarding [10] were very useful.

References

1. J. Berger *et al.*, Phys. Rev. Lett. **61** (1988) 919
2. B. Mayer *et al.*, Phys. Rev. **C53** (1996) 2068
3. C. Wilkin, Phys. Rev. **C47** (1993) R938
4. K. Kilian and H. Nann, AIP Conf. Rep. **221** (1990) 185
5. G. Fäldt and C. Wilkin, Nucl. Phys. **A587** (1995) 769
6. A.M. Bergdolt *et al.*, Phys. Rev. D **48** (1993) R2969; A. Taleb, PhD thesis, Université Louis Pasteur, Strasbourg (1994) (CRN 94-61); F. Hibou *et al.*, Phys. Lett. B **438** (1998) 41; F. Hibou *et al.*, Phys. Rev. Lett. **83** (1999) 492
7. C. Caso *et al.*, Eur. Phys. J. **C3** (1998) 1
8. F. Plouin *et al.*, Phys. Lett. B **276** (1992) 526
9. N. Willis *et al.*, Phys. Lett. B **406** (1997) 14
10. U. Tengblad, TSL/ISV Report 96-0163, 1996 (unpublished)
11. J. Carbonell and M. Mangin-Brinet, private communication (1999)
12. G. Fäldt and C. Wilkin, Phys.Lett. **B382** (1996) 209
13. H. Rohdjess *et al.*, Phys. Rev. Lett. **70** (1993) 2864
14. V.N. Nikulin *et al.*, Phys. Rev. **C54** (1996) 1732